

# Epigallocatechin-3-gallate Delivered in Nanoparticles Increases Cytotoxicity in Three Breast Carcinoma Cell Lines

Fulvia Farabegoli,\* Andreia Granja, Joana Magalhães, Stefania Purgato, Manuela Voltattorni, and Marina Pinheiro



Cite This: <https://doi.org/10.1021/acsomega.2c01829>



Read Online

ACCESS |



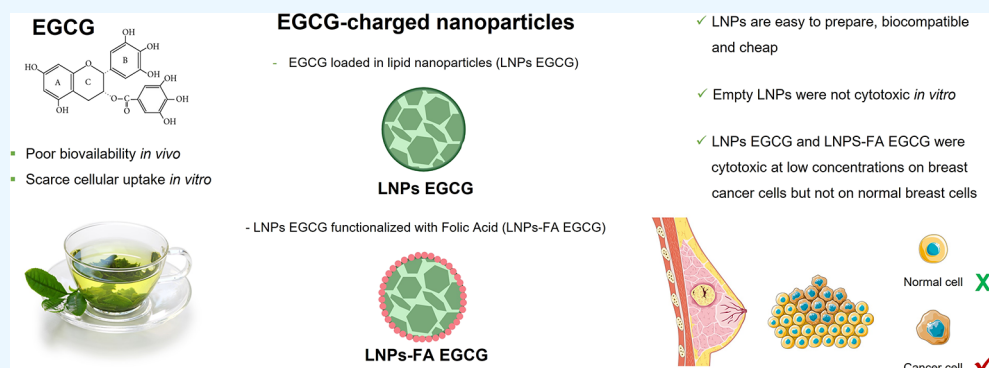
Metrics & More



Article Recommendations



Supporting Information



**ABSTRACT:** The anticancer activity of epigallocatechin-3-gallate (EGCG), orally administered, is limited by poor bioavailability, absorption, and unpredictable distribution in human tissues. EGCG charged nanoparticles may represent an opportunity to overcome these limitations. We assayed two different kinds of lipid nanoparticles (LNPs and LNPs functionalized with folic acid) charged with EGCG on three breast carcinoma cell lines (MCF-7, MDA-MB-231, and MCF-7TAM) and the human normal MCF10A mammary epithelial cells. Both LNPs loaded with EGCG, at low concentrations, induced a significant cytotoxicity in the three breast carcinoma cells but not in MCF10A cells. In view of a future application, both LNPs and LNPs-FA were found to be very suitable for *in vitro* studies and useful to improve EGCG administration *in vivo*. Since they are produced by inexpensive procedures using bioavailable, biocompatible, and biodegradable molecules, they represent an applicable tool for a more rationale use of EGCG as an anti-cancer agent.

## INTRODUCTION

Green tea is one of the most popular beverages in the world; consuming green tea is considered as a health-promoting habit due to its well-known antioxidant, anti-inflammatory, and chemopreventive activities.<sup>1,2</sup> Green tea consumption has beneficial effects on many human diseases, including obesity, metabolic syndrome, neurodegenerative disorders, inflammatory diseases, and cancer.<sup>3–5</sup> These properties depend on a family of polyphenol molecules, named catechins, present in green tea, with epigallocatechin-3-gallate (EGCG) being the most abundant and active. One of the most significant limitations to a broad use of EGCG in human health is its scarce absorption and bioavailability. After oral administration, green tea catechins (GTC) are mainly metabolized by phase 2 enzymes: methylation, sulphatation, and glucuronidation occur in the intestine and liver. A large amount of catechins is further catabolized by microflora in the colon, reabsorbed into plasma, and eliminated through urine.<sup>6–8</sup> The final concentration of GTC, including EGCG, is very low in blood and tissues, barely around micromolar concentrations, varying among individu-

als.<sup>9,10</sup> Despite the very low concentration of GTC in the tissues after oral administration, well-targeted chemoprevention studies in human cancer such as prostate,<sup>11</sup> breast,<sup>12</sup> colon<sup>13</sup> have demonstrated the potentiality of GTC use. Breast carcinoma is a suitable model where the delivery of GTC by nanoparticles might be applied: this pathology has a high social impact, and it is often early detected; it also presents a high rate of response to therapy and long intervals free of disease even in the case of relapse. Improvement in GTC absorption and distribution might give a significant enhancement to the use of GTC as a chemopreventive and therapeutic agent in breast cancer. Nanotechnology applied to medicine is emerging as an innovative and leading strategy in drug delivery.<sup>14</sup> Recent

Received: March 25, 2022

Accepted: July 15, 2022

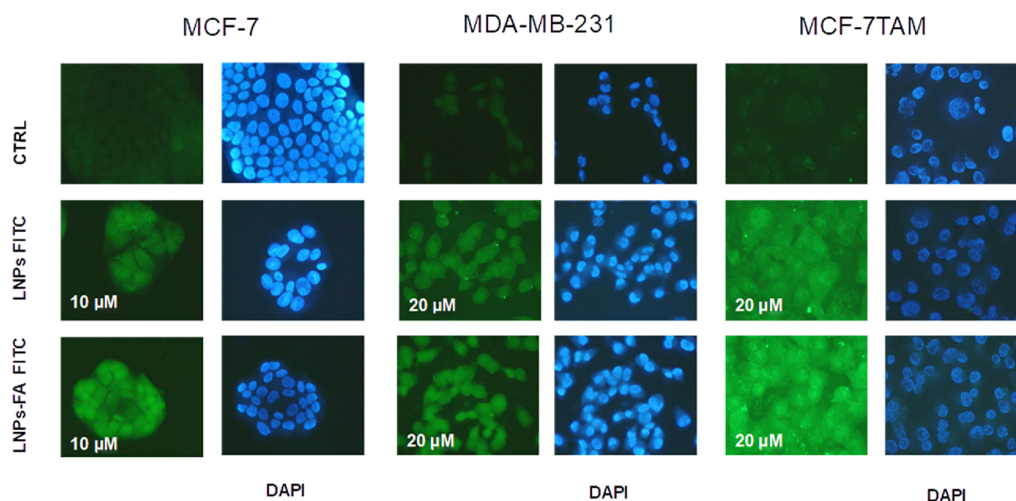


**Figure 1.** LNPs FITC and LNPs-FA FITC uptake in MCF-7, MDA-MB-231, and MCF-7TAM cells. Control (CTRL) and 2 h LNPs FITC- and LNPs-FA FITC-treated MCF-7, MDA-MB-231, and MCF-7TAM cells. 10 and 20  $\mu\text{M}$  are the concentrations used. The cells were fixed in 1% formalin for 15 min and stained by DAPI.

advances in this field have demonstrated that nanoparticles loaded with EGCG might overcome the metabolic changes and the distribution variability of catechins in humans.<sup>15</sup> Lipid nanoparticles (LNPs), particularly, are a promising type of nanodelivery system due to their low-cost production, easy scale-up, high stability, and biocompatibility.<sup>16</sup> Additionally, the surface of these nanoparticles can be easily modified. It is therefore possible to enhance their cancer cell specificity by surface functionalization with several ligands, such as folic acid (FA), to target the folate receptor that is overexpressed in several cancer cell subtypes.<sup>17–19</sup>

In the present study, the *in vitro* effects of LNPs and FA-functionalized LNPs loaded with EGCG were investigated on three breast carcinoma cell lines (MCF-7, MDA-MB-231, and MCF-7TAM) and in one normal immortalized breast cell line (MCF10A) to assay and compare the efficacy in view of a future effective delivery. MCF-7, MDA-MB-231, and MCF-7TAM cell lines were selected as representative of different carcinomas, showing peculiar genetic and bio-pathologic profiles, corresponding to patients who undergo different pharmacologic treatments and have different outcomes. The MCF-7 cell line is representative of the most common type of breast cancer, which shows estrogen receptor  $\alpha$  (ER $\alpha$ ) overexpression and is treated by Tamoxifen or anti-estrogen drugs. The MCF-7-derived Tamoxifen-resistant cell line corresponds to the breast neoplasms that may arise in patients who relapse after anti-endocrine therapy and show aggressive features. Lack of both specific markers and targeted therapies distinguish the triple-negative breast carcinoma, the less curable of all, well represented by the MDA-MB-231 cell line.<sup>20</sup> We studied whether the three cancer cell lines might be differently sensitive to LNPs charged with EGCG, delivered in different types of nanoparticles.<sup>21</sup> Cytotoxic effects on breast normal cells were also studied to verify EGCG and nanoparticle safety. By means of this feasibility study, we intended to set the prerequisite for future applications of lipid-based NPs that are emerging as a promising drug delivery tool.

## RESULTS

The sizes of the LNPs used in this study were 333 and 313 nm in the case of nonfunctionalized and functionalized LNPs, with the

polydispersity index (PI) of both formulations being below 0.2, confirming that the NPs populations are monodisperse. The  $\zeta$  potentials were  $-31$  and  $-30$  mV in the case of non-functionalized and functionalized LNPs, respectively. These values are characteristic of highly stable nanoformulations in suspension. The encapsulation efficiencies (EE) were 96% (for nonfunctionalized LNPs) and 85% (for functionalized LNPs), while the loading capacities (LC) were 2.6 and 2.3, respectively. Moreover, regarding the morphology of the NPs, the transmission electron microscopy (TEM) photographs demonstrated that the LNPs presented a spherical regular morphology.<sup>19</sup> Concerning the EGCG release experiments, both formulations, *i.e.*, functionalized and nonfunctionalized, demonstrated a sustained release of EGCG, being released with less than 20% in both formulations after 5 h and less than 40% after 24 h in acidic pH values. Finally, both formulations are physico-chemically stable and maintained their characteristics, with their size, charge, and LC unchanged for at least 2 months.<sup>15,22</sup> In this study, MCF-7, MDA-MB-231, MCF-7TAM, and MCF10A cells were treated with LNPs labeled with FITC at different concentrations (5–20  $\mu\text{M}$ ) for 2, 6, or 16 h. These incubation times were considered suitable to verify the LNPs intake, which was supposed to occur in a short time. The concentrations were selected on the bases of previous studies conducted by us onto the same cell types treated with various free EGCG concentrations.<sup>23,24</sup> We deliberately used low EGCG concentrations, expected to be scarcely cytotoxic or with no cytotoxic effect, for a better comparison between free and nanodelivered EGCG. A fluorescence increase was detectable after 2 h in MCF-7, MDA-MB-231, and MCF-7TAM cells treated with LNPs FITC and LNPs-FA FITC in contrast with control cells (CTRL) that did not receive any treatment (Figure 1). MCF10A cells, treated with 10  $\mu\text{M}$  LNPs FITC, showed fluorescence superimposable to CTRL cells, whereas LNPs-FA FITC treatment resulted in a modest increase in cytoplasm fluorescence (Supporting Information, Figure S1). The most suitable concentrations found were 10  $\mu\text{M}$  for MCF-7 and MCF10A and 20  $\mu\text{M}$  for MDA-MB-231 and MCF-7TAM cells. The shortest time of treatment (2 h) found to be effective in nanoparticles' intake was used to evaluate the cytotoxic effects.

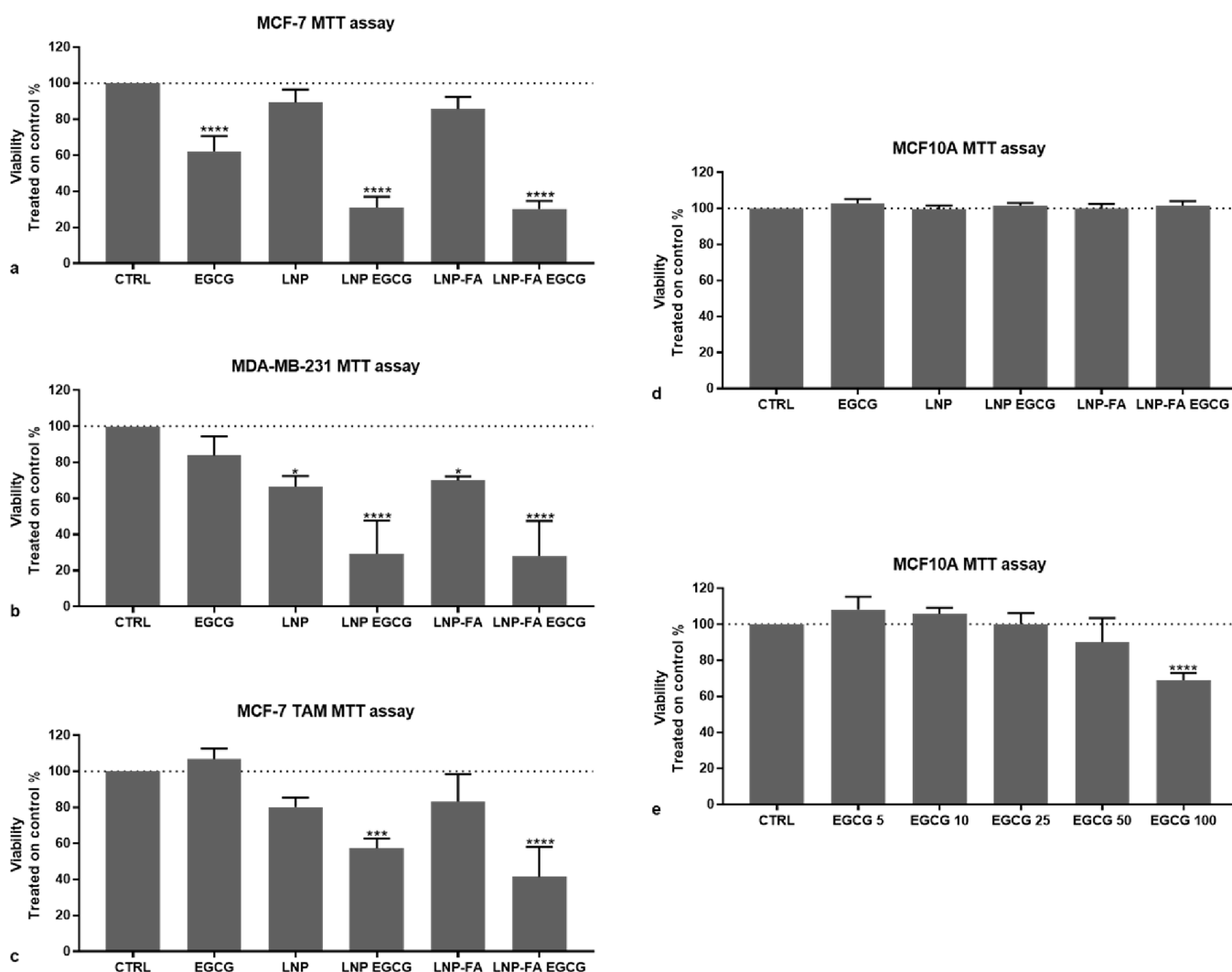


**Figure 2.** MTT assay on (a) MCF-7, (b) MDA-MB-231, (c) MCF-7TAM, and (d) MCF10A cells. Control cells (CTRL). The cells were treated with 10  $\mu$ M (MCF-7 and MCF10A) and 20  $\mu$ M (MDA-MB-231 and MCF-7TAM cells) for 2 h. Then, the medium was changed and the MTT assay was performed after further 70 h. (e) MTT assay after 5, 10, 20, 50, and 100  $\mu$ g/mL EGCG treatments on MCF10A cells for 72 h. The values were normalized to the untreated controls. The results are expressed as average  $\pm$  SE of three independent experiments. \* $p$  < 0.05; \*\* $p$  < 0.01; \*\*\* $p$  < 0.001; \*\*\*\* $p$  < 0.0001.

MCF-7, MDA-MB-231, and MCF-7 TAM cells were treated with LNPs, LNPs-FA, LNPs EGCG, LNPs-FA EGCG, and free EGCG at different concentrations: 10  $\mu$ M (MCF-7 and MCF10A) and 20  $\mu$ M (MDA-MB-231 and MCF-7TAM cells) for 2 h. Then, the medium was changed, and the cells were allowed to grow until 72 h since the experiment started, and the cell viability was analyzed. As shown in Figure 2a, a significant cytotoxic effect was found in MCF-7 cells after EGCG treatment ( $p$  < 0.0001), whereas MDA-MB-231 (Figure 2b) and MCF-7TAM cells (Figure 2c) did not show any viability decrease. In contrast, when the cells were treated with both LNPs EGCG and LNPs-FA EGCG, the cytotoxicity dramatically increased in all the three cell lines. Viability dropped around 30% after both LNPs EGCG and LNPs-FA EGCG treatments in MCF-7 and MDA-MB-231 cells; LNPs-FA EGCG was more effective than LNPs EGCG in MCF-7TAM cells (41.4 and 57.3%, respectively). MCF10A cells showed a lower sensitivity to LNPs than the cancer cell lines: 10  $\mu$ M free EGCG or 10  $\mu$ M LNP did not show cytotoxic effects (Figure 2d) as well as after free EGCG treatments: a significant viability decrease was only detected after 100  $\mu$ M EGCG treatment for 72 h (Figure 2e).

Empty nanoparticle (LNPs and LNPs-FA) treatments produced a limited but not statistically significant reduced viability in breast cancer cell lines (Figure 2a–c) and no effect on MCF10A cells (Figure 2d).

To better improve the cytotoxicity analysis after treatment with LNPs and LNPs-FA, we repeated the viability assay by using Phasefocus Livecyte, a technology that enables monitoring growing cells by a camera and evaluating both the cell number and/or the area occupied by cells during the time course. The cells were treated for 2 h with the different nanoformulations and free EGCG at the concentrations used for the MTT assay. After washing with PBS and replacing the medium, the 96-multiwell plate was placed into the Livecyte incubator. The images were taken every 40 min for the following 70 h, resulting in overall 72 h experimental time. At the end, the multiwell plate was removed and the MTT assay was run, and the data were compared. Livecyte analysis confirmed the strong cytotoxic effect of EGCG when conveyed in cells by both LNPs and LNPs-FA (Figure 3).

As shown in Figure 3a, the proliferation curves based on the number of MCF-7 cells clearly defined a strong gap between

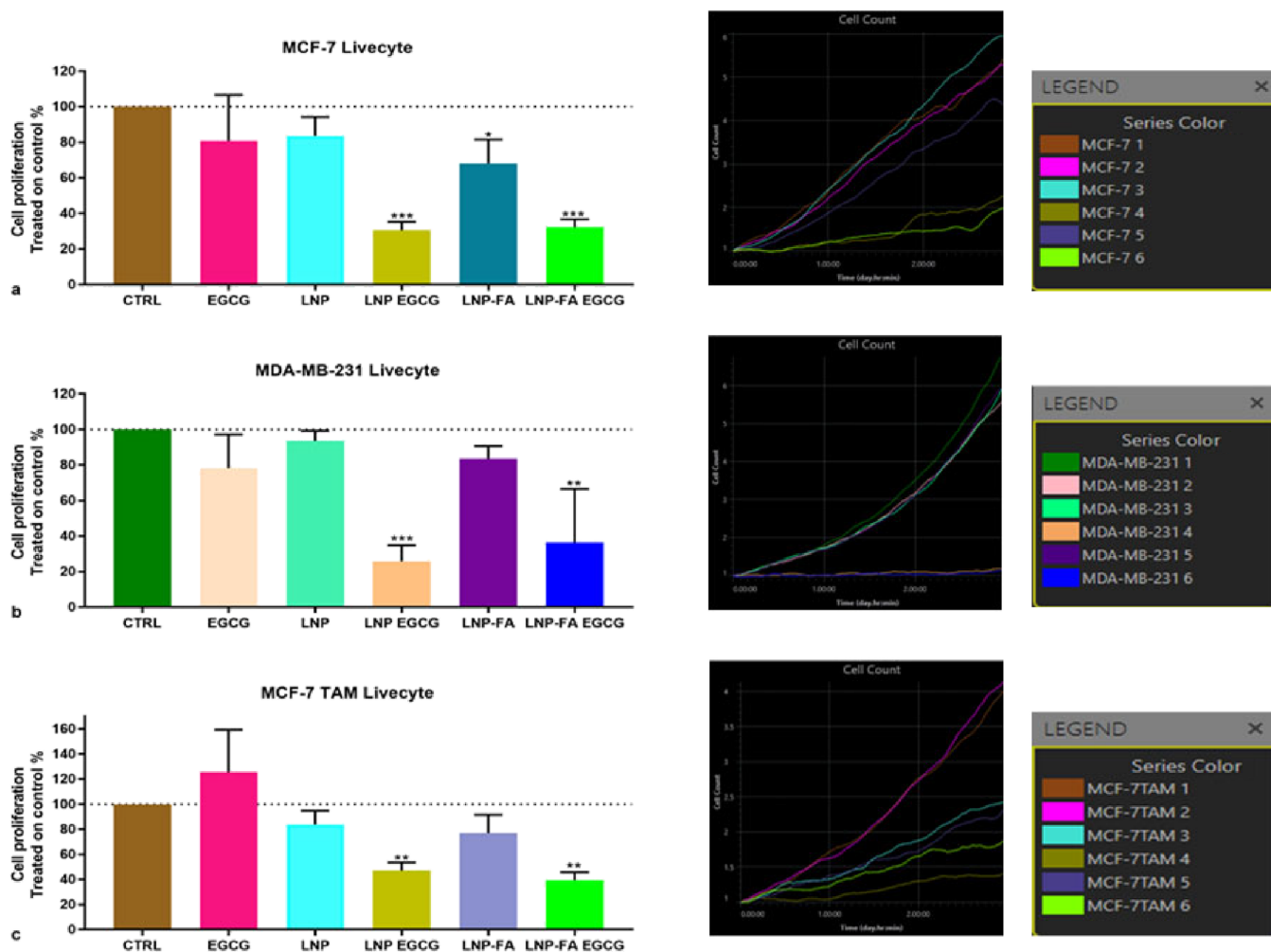


**Figure 3.** Liveocyte analysis of (a) MCF-7, (b) MDA-MB-231, and (c) MCF-7TAM cell growth. Control cells (CTRL). The cells were treated with 10  $\mu\text{M}$  (MCF-7) and 20  $\mu\text{M}$  (MDA-MB-231 and MCF-7TAM cells) for 2 h. Then, the medium was changed and Liveocyte analysis was performed for 70 h, resulting in overall 72 h experimental time. The cells were counted every 40 min in the field of view (FOV) and the number of cells recorded at the end of the experiment was used for statistical analysis. 1 (CTRL), 2 (EGCG), 3 (LNPs), 4 (LNPs EGCG), 5 (LNPs-FA), and 6 (LNPs-FA EGCG). The values were normalized to the untreated controls. The results are expressed as average  $\pm$  SE of three independent experiments. \* $p < 0.05$ ; \*\* $p < 0.01$ ; \*\*\* $p < 0.001$ ; \*\*\*\* $p < 0.0001$ .

CTRL (1), EGCG (2)-, LNPs (3)-, LNPs-FA (5)-, LNPs EGCG (4)-, and LNPs-FA EGCG (6)-treated cells. The curves are the result of the numerical count of cells. According to Liveocyte detection, LNPs-treated cells grew faster followed by EGCG and CTRL and then FA-LNPs. LNPs EGCG and LNPs-FA EGCG treatments were significantly cytotoxic ( $p < 0.001$ ) (Figure 3a). These differences were even more defined in MDA-MB-231 cells (Figure 3b), having a proliferation profile like MCF-7 cells. In this case, the curve at the top corresponds to CTRL cells (1). LNPs EGCG (4) and LNPs-FA EGCG (6) treatments impaired cell proliferation with a great efficacy. In contrast, MCF-7TAM cells showed a greater sensitivity to LNPs and LNPs-FA, which impaired the cell growth (Figure 3c), although a significant difference was found between LNPs and LNPs-FA and LNPs EGCG and LNPs-FA EGCG ( $p < 0.05$ ) (Figure 3c). The videos showing the cell growth in CTRL and treated cells are available in the Supporting Information as Video S1 (MCF-7), Video S2 (MDA-MB-231), and Video S3 (MCF-7TAM). By the analysis of the videos, we found that, after empty nanoparticle treatments, cell proliferation slowdown occurred and it caused a modest cell number decrease, whereas cell death occurred in LNPs EGCG- and LNPs-FA EGCG-treated

samples. The MTT assay after Liveocyte incubation also confirmed that cell viability was significantly impaired when EGCG was loaded into LNPs and LNPs-FA (Figure 4), although both unloaded nanoparticles (LNPs and LNPs-FA) showed a significant reduction of cell viability in MDA-MB-231 cells with respect to the CTRL.

We also analyzed the MCF10A cell response to treatments by Phasefocus Liveocyte. Both the cell number and confluence showed the cell growth increase with respect to CTRL cells, with the only exception of LNPs-FA treatment. Overall, no significant cytotoxicity was detected after both empty and EGCG-loaded nanoformulation treatments (Supporting Information Figure S2).

An Annexin V-FITC/PI assay, as detected by flow cytometry (FCM), was applied to those samples that showed a significant viability decrease and cell death (LNPs EGCG- and LNPs-FA EGCG-treated cells). The Annexin V-FITC positive cells indicate early apoptosis (EA), whereas late apoptosis (LA) corresponds to cells labeled by both Annexin V-FITC and PI. PI only staining indicates necrosis. The results are shown in Figure 5a,b.



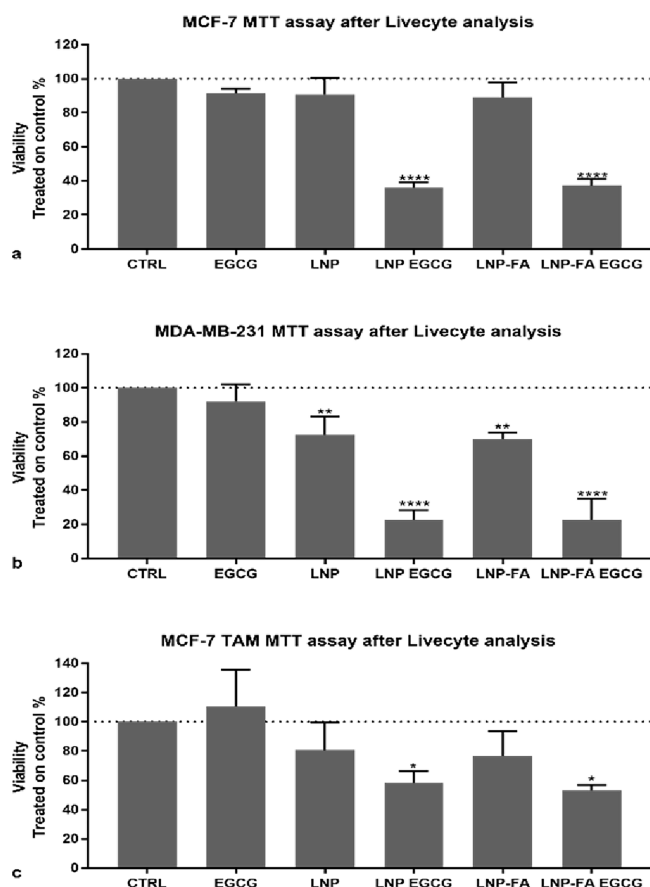


**Figure 4.** MTT assay after Livecyte analysis. (a) MCF-7, (b) MDA-MB-231, and (c) MCF-7TAM cells. Control cells (CTRL). The cells were treated with 10  $\mu\text{M}$  (MCF-7) and 20  $\mu\text{M}$  (MDA-MB-231 and MCF-7TAM cells) for 2 h. The MTT assay was run after Livecyte analysis (overall 72 + 5 h). The values were normalized to the untreated controls. The results are expressed as average  $\pm$  SE of three independent experiments. \* $p < 0.05$ ; \*\* $p < 0.01$ ; \*\*\* $p < 0.001$ ; \*\*\*\* $p < 0.0001$ .

In MCF-7 treated cells, the increase in EA and LA with respect to CTRL cells was very scarce after LNPs EGCG treatments, whereas it increased after LNPs-FA EGCG treatments ( $p < 0.01$ ). PI positive cell numbers did not change significantly. In contrast, MDA-MB-231 showed an early and significant increase in apoptosis after LNPs EGCG treatment for 24 h ( $p < 0.05$ ). Annexin V-FITC-labeled cells (EA and LA) increased after 24 h ( $p < 0.05$ ) and 48 h ( $p < 0.01$ ) of LNPs-FA EGCG treatments in MCF-7TAM cells.

## DISCUSSION

EGCG nanodelivery is a suitable strategy to verify whether different breast carcinoma cell types might be differently sensitive to EGCG, independent of all the “*in vitro*” conditions, which make EGCG intake variable and unpredictable. We used two different types of LNPs to detect possible differences in intake and effects. We also treated normal breast cells to verify any cytotoxic effect.

In spite of the differences among the three cell lines, all of them were found to be sensitive to low concentrations of EGCG delivered in both LNPs types. The most interesting finding was that MDA-MB-231 cells, representative of one of the most aggressive forms of breast cancer, named triple-negative, were very sensitive to EGCG loaded in both LNPs treatments. As a

confirmation of the strong cytotoxic effect, apoptosis was significantly detected as an early change in this cell lines. MCF-7TAM cells, representative of Tamoxifen-resistant tumors, which are difficult to be treated as well, showed a good response to EGCG treatment. As these types of breast carcinoma lack any specific therapy, the robust cytotoxic effect found makes EGCG vehiculated by LNPs a valuable molecule to be taken into consideration for chemoprevention and therapy. Many studies reported significant differences in concentrations and efficacy of EGCG treatments in the same cell lines used in different laboratories.<sup>25</sup> We considered that the “*in vitro*” study of EGCG loaded in LNPs could be assumed as more reliable than free EGCG administration. The cytotoxic effects that we detected in different cell lines was only attributable to EGCG activity since cell death was found in LNPs EGCG- and LNPs-FA EGCG-treated samples, whereas empty LNPs induced the transient cell proliferation slowdown.

We used low EGCG concentrations as a deliberate decision, which was based on our long experience about the effects of free EGCG on MCF-7, MDA-MB-231, and MCF-7TAM cell lines grown by us for many years.<sup>23,24</sup> Furthermore, our previous published data demonstrate that nanoformulations up to concentrations of 25  $\mu\text{M}$  of EGCG did not compromise cell viability in Caco-2 cell lines.<sup>19</sup> Therefore, two different concentrations below 25  $\mu\text{M}$  were chosen in this study. We considered that low EGCG concentrations might clearly reveal any greater effect of EGCG delivered into LNPs with respect to free EGCG. In fact, only in one case (MTT assay, Figure 2), free EGCG treatment resulted in a significant cytotoxic effect on MCF-7 cells, whereas a significant viability decrease was only found in all the three cell lines after LNPs EGCG and LNPs-FA EGCG treatments.

We can confirm that EGCG do not harm normal cells, either delivered in LNPs or free. At these concentrations, both the LNPs preferentially entered cancer cells whereas they were poorly assumed by normal cells. We can only speculate that a different membrane composition in neoplastic and normal cells might explain this finding.<sup>26,27</sup> Lack of harmful effects is an ideal characteristic for any cancer therapeutic intervention, and this finding supports EGCG as a suitable molecule to this aim.

To define the schedule of experiments, we tested various times of incubation of both LNPs and LNPs-FA loaded with FITC (2, 4, 6, and 16 h), but we used the shortest time of incubation that resulted in an increase in cell fluorescence. We considered that in an “*in vivo*” administration of LNPs, they are rapidly uptaken by responsive cells, whereas the remaining LNPs are transported and degraded progressively.<sup>21</sup> Folic acid-functionalized nanoparticles were also found to be significantly concentrated into tumor cells after 1–4 h.<sup>28</sup> Altogether, these data suggested to treat the cells for a short time. MTT and Livecyte experiments followed the same protocol and were run separately: after 2 h treatments, the medium was replaced and the cells were grown for further 70 h. The results were comparable. For further confirmation, one more MTT assay was run after Livecyte: the plates were taken out of the instrument and incubated for 4 h with MTT and 1 h with DMSO. In this case only, the overall experimental time was 77 h.

We used two different nanoparticles (LNPs and LNPs-FA), supposed to be assumed by cells by different mechanisms, since we intended to define which kind of EGCG administration might be more suitable in the three breast cancer cell lines. Nanoparticles can enter cells via several ways, including endocytosis (clathrin- or caveolae-mediated), non-endocytic

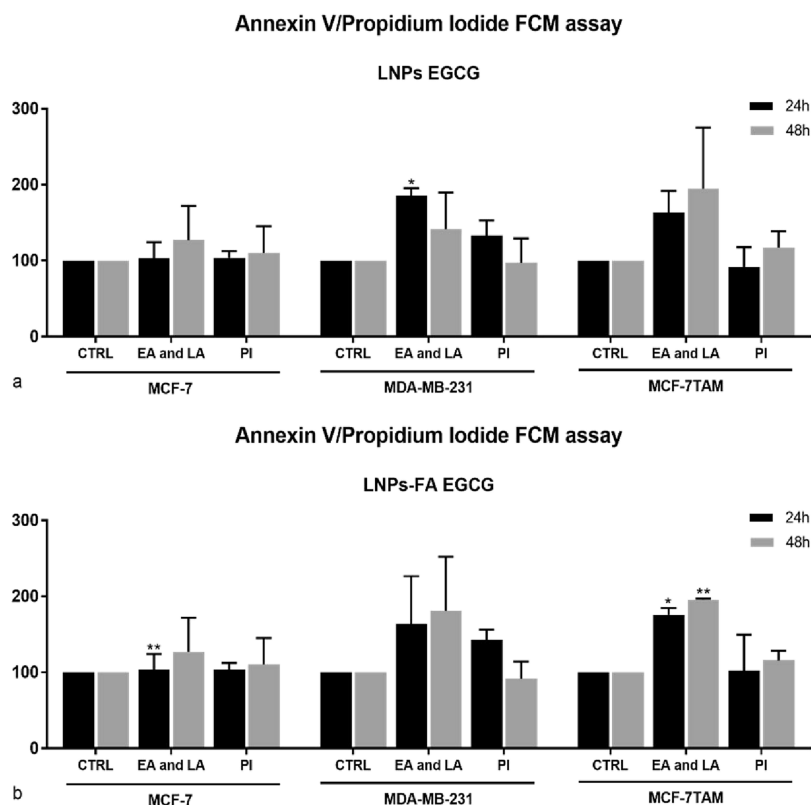


**Figure 5.** Annexin V/propidium iodide staining. MCF-7, MDA-MB-231, and MCF-7TAM cells. The cells were treated with 10  $\mu\text{M}$  (MCF-7) and 20  $\mu\text{M}$  (MDA-MB-231 and MCF-7TAM cells) with (a) LNP EGCG and (b) LNP-FA EGCG for 2 h. Then, the medium was replaced and the samples were analyzed by FCM 24 and 48 h later. Control cells (CTRL), early apoptosis (EA), late apoptosis (LA), propidium iodide (PI). The values were normalized to the untreated controls. The results are expressed as average  $\pm$  SE of two independent experiments. \* $p < 0.05$ ; \*\* $p < 0.01$ ; \*\*\* $p < 0.001$ ; \*\*\*\* $p < 0.0001$ .

pathways, macropinocytosis, and phagocytosis.<sup>29</sup> Functionalization with FA is a current strategy to target cancer cells having a great FA receptor expression at the surface of the cells. These two different approaches were compared but, on one hand, the apparent more efficient intake of LNPs-FA FITC was not responsible for a different cytotoxicity after LNPs EGCG and LNPs-FA EGCG treatments. According to the MTT and Livecyte data, viability after treatments with LNPs EGCG or LNPs-FA EGCG was superimposable in all the cell lines but MCF-7TAM cells. We expected that MDA-MB-231 cells could intake a greater quantity of LNPs-FA since triple-negative breast carcinoma patients are reported to have abundant expression of FA receptors and are considered suitable candidates for an FA-targeted treatment.<sup>30,31</sup> In contrast, MCF-7TAM cells revealed a greater sensitivity to EGCG delivered by LNPs-FA. We cannot presently explain this result, but we can speculate that during the development of the drug-resistant phenotype, the FA receptor expression might increase. FA is a strong supporter of cell proliferation<sup>32</sup> and cancer signaling pathways such as AKT/ERK, a pathway very active in Tamoxifen-resistant MCF-7TAM cells.<sup>23</sup> On the bases of the present results, LNPs might be efficiently used independent of the abundance of FA receptors in the target cells, although breast cancer cells rich in FA receptors might be preferentially targeted with respect to normal cells.<sup>29,30</sup> Both the different uptake and safety of EGCG might concur to explain the differences found in cytotoxicity after free EGCG, LNPs EGCG, and LNPs-FA EGCG treatments, with EGCG being nontoxic to human normal cells of various tissues.<sup>33,34</sup> A MCF10A cell viability decrease was only detected after 100  $\mu\text{g}/$

mL EGCG treatment, a concentration rather high and not advisable for any potential treatment.

The comparison between MTT and Livecyte analysis did not present inconsistencies. The videos clearly demonstrated that cell proliferation was not arrested by empty nanoparticle treatments. A modest decline of cell proliferation was detected in MCF-7TAM cells, which showed a lower proliferation rate after LNPs and LNPs-FA treatments, in comparison to CTRL and EGCG-treated samples. As shown in the videos, MDA-MB-231 and MCF-7TAM cells moved into the well, changing the number of cells counted in FOV with respect to the initial population. In contrast, MCF-7 cells grew close to each other and did not move. However, the Livecyte camera might mislead in defining the outline of each cell. The comparison of the two graphs (number of cells and confluence area) represents a good tool for the correct evaluation of the experiment. The strong point of Livecyte analysis is that it avoids mistakes due to handling: then, the set of data can be considered highly reliable. The MTT assay run after Livecyte also validated the results: good agreement was found with Livecyte data. Differences in the percentage of viable cells recorded by the two assays should take into account that MTT is a test based on a metabolic activity and the optical density value is the result of the evaluation of all the cells into each well. In contrast, Livecyte analysis is performed selecting a defined area (1 mm  $\times$  1 mm) and the number of cells and/or the confluence area is measured.

Flow cytometry analysis after 24 and 48 h treatments detected apoptosis and no necrosis in MCF-7, MDA-MB-231, and MCF-7TAM cells. Apoptosis occurred quite early (24 h) in MCF-7,

MDA-MB-231, and MCF-7TAM cells and was only detectable later (48 h) in MCF-TAM cells after LNPs-FA EGCG treatment. Probably, the cell proliferation decreased and was followed by a slow rate of cell death. In contrast, CTRL, EGCG-, LNPs-, and LNPs-FA-treated samples went on in cell cycling increasing the number of cells and progressively filling the bottom of the wells, as shown in the videos and demonstrated by the data evaluation based on the number of cells. With respect to MCF-7 cells, a faster rate of cell death occurred in MDA-MB-231 and MCF-7TAM cells. It is intriguing that, in contrast with the supposed richness of FA receptors in MDA-MB-231 cells, we found that apoptosis was triggered by LNPs EGCG treatment, whereas MCF-7 and MCF-7TAM cells showed apoptosis after LNPs-FA EGCG treatment. This finding needs to be further defined.

## CONCLUSIONS

By the present study, we confirm that EGCG conveyed by LNPs is a suitable tool to investigate EGCG activity for future “*in vivo*” applications as an anti-cancer agent. Lack of cytotoxic effects at the investigated concentrations in normal cells further supports this potentiality. *In vitro* studies have been diriment to define the molecular targets of EGCG, and they still have a fundamental role in detecting neoplasms and molecules sensitive to EGCG activity.<sup>35–37</sup> EGCG loaded in LNPs represents an opportunity to better define the EGCG mechanisms of action and to address the chemoprevention activity toward proper targets with improved efficiency and without side effects.<sup>38–40</sup> These LNPs show many advantages, such as an easy and inexpensive large-scale production and sterilization, high biocompatibility and biodegradability, improved bioavailability, controlled release of drugs, and high efficiency in drug targeting.<sup>16,19,41,42</sup> With this approach, the pharmacokinetic properties of EGCG may be potentiated by protecting it from premature degradation and prolong its circulation time and simultaneously target cancer cells, following the concept of nano-chemoprevention proposed by Siddiqui and co-workers.<sup>43</sup>

## METHODS

**LNPs Characteristics.** The LNPs were produced by high-shear homogenization and ultra-sonication techniques.<sup>16</sup> A solid lipid (Precirol ATO 5), liquid lipid (Mygliol 812), and surfactant (Tween 60) were heated in a water bath at 70 °C until the solid lipid melted. Preheated ultrapure water was added to the lipid phase followed by stirring in an ultraturrax (Ystral X10/20 E3; Ballrechten-Dottingen, Germany) at 822g for 30 s and ultrasonication (VCX130, Sonics and Material Vibra-Cell™ with a CV-18 probe; 115 Newtown CT, USA) at an amplitude frequency of 70% for 5 min. The nanoemulsion was then cooled at room temperature (25 °C) and stored at 4 °C until further use. The size of the NPs, the polydispersity index (PI), and the  $\zeta$  potential were determined by dynamic light scattering (Brookhaven Instruments Corporation, Holtsville, NY, USA). For the production of EGCG-loaded LNPs, EGCG was dissolved in the aqueous phase and added to the lipid phase in a similar manner to previously described. Production of FA-functionalized LNPs was performed by adding the DSPE-PEG2000-FA ligand<sup>42</sup> to the lipid phase in a ratio of 1% w/w of total formulation mass. The encapsulation efficiency (EE) and the loading capacity (LC) were measured by UV/vis spectrophotometry using an indirect method. EE corresponds to the percentage of EGCG that is entrapped in the lipid NPs in

relation to the initial amount used, while LC is the amount of EGCG per unit weight of the total NPs mass.

The morphology of the LNPs was studied by transmission electron microscopy (TEM).<sup>19</sup>

**Cell Lines.** MCF-7 and MDA-MB-231 were purchased from the American Type Culture Collection (Rockville, MD, USA) and maintained in E-MEM (MCF-7) or DMEM (MDA-MB-231) supplemented with 10% fetal bovine serum (FBS), 2 mM L-glutamine, 500 U/mL penicillin, and 50  $\mu$ g/mL streptomycin. The MCF-7TAM cell line was established by growing MCF-7 cells in MEM medium (without phenol red and with charcoal-treated 10% FBS) containing  $10^{-7}$  M 4-OH-tamoxifen as already described.<sup>23,24,44</sup> MCF10A was purchased from the American Type Culture Collection (Rockville, MD, USA) and maintained in low glucose DMEM medium, supplemented with 20% fetal bovine serum (FBS), 2 mM L-glutamine, 500 U/mL penicillin, 50  $\mu$ g/mL streptomycin, insulin (25 U), hydrocortisone (0.5  $\mu$ g/mL), and EGF (5 nM).

**LNPs Intake in MCF-7, MDA-MB-231, MCF-7TAM, and MCF10A Cells.** Evaluation of LNPs intake in MCF-7, MDA-MB-231, MCF-7TAM, and MCF10A cells was performed with fluorescein isothiocyanate (FITC)-labeled nanoparticles that were developed replacing EGCG with FITC. FITC was dissolved in the lipid phase (2% w/w of the lipid mass). The cells (50,000 for well) were plated in a 24-multiwell plate with sterile coverslips as a support and were allowed to attach and grow for at least 24 h. The cells were treated with LNPs FITC and LNPs-FA FITC at different concentrations (5–20  $\mu$ M) for 2, 6, or 16 h. Then, the medium was replaced and the samples were fixed in 1% formalin in 1 $\times$  PBS for 15 min and finally mounted in a solution of 4',6-diamidino-2-phenylindole DAPI (0.2  $\mu$ g/mL) in 1,4-diazabicyclo[2.2.2]octane (DABCO). The samples were viewed with a Nikon fluorescence microscope equipped with a filter for FITC and DAPI.

**MTT and Livecyte Assay.** The MTT assay was performed by seeding the cells onto 96-well plates (4000 cells for well) in medium. 4-OH-tamoxifen ( $10^{-7}$  M) was added to MEM medium for growing MCF-7TAM cells. The day after the cells were incubated with different concentrations (10  $\mu$ M MCF-7 and MCF10A and 20  $\mu$ M MDA-MB-231 and MCF-7TAM) of LNPs, LNPs-FA, LNPs EGCG, LNPs-FA EGCG, and free EGCG for 2, 16, or 24 h. After incubation, the medium was replaced, and the cells were allowed to grow for 72 h from the treatment time. Cell viability experiments were conducted in triplicate, and at least three independent experiments were carried out. MTT was added to each well from a stock solution (10  $\mu$ L from 5 mg/mL in PBS in 100  $\mu$ L medium for each well) and incubated for 4 h at 37 °C in the incubator. Then, the medium was aspirated and replaced with 100  $\mu$ L of DMSO. After 1 h, the absorbance in each well was measured with a microplate reader (Beckton Dickinson, Boston, MD, USA) at 570 nm. In a second set of experiments, the MTT assay was performed after Phasefocus Livecyte analysis as a comparison and validation. The MTT assay was run immediately at the end of the Phasefocus Livecyte incubation as previously described.

Phasefocus Livecyte is a kinetic cytometer equipped with a quantitative phase imaging modality that enables users to obtain fluorescence-like high-contrast images without the need of any labels. Cell proliferation measurements such as cell count, confluence, and cell doubling times are automatically determined and displayed on the proliferation dashboard. Additionally, Livecyte measures cell dry mass, a unique Quantitative Phase Imaging (QPI) property that independently



quantifies cell growth from cell division events. QPI produces high-contrast images, with cells appearing as bright objects on a dark background since it records the phase information of light passing through the cell, generating pixel values and therefore images. The cell number and confluence area can be measured at each step and contribute to generate the final curves.<sup>45</sup> Technical notes and a more detailed description of the instrument are available at the website: <https://www.phasefocus.com/livecyte>.

All the experiments were performed in 96-well plates. The cells (4000 for well) were seeded in triplicate and allowed to grow overnight. The day after, they were treated with free EGCG, LNPs, LNPs-FA, LNPs EGCG, and LNPs-FA EGCG at different concentrations: MCF-7 and MCF10A (10  $\mu$ M), MDA-MB-231 and MCF-7TAM cells (20  $\mu$ M). After 2 h incubation, the medium was discarded and replaced with fresh medium. Then, the plate was transferred in the Livecyte incubator at 37 °C with 5% CO<sub>2</sub> and 95% humidity. High-contrast quantitative phase images were automatically captured. Cells were imaged with an Olympus PLN 10 $\times$  (0.25 NA) objective and 1 mm  $\times$  1 mm field of view (FOV) per well for 70 h at 40 min intervals. Overall, the experimental time was 72 h. Both the cell count and cell confluence (area) were recorded and measured by the instrument every 40 min, reported in an Excel file, and then used for further elaboration.

**Apoptosis Detection by the Annexin V-Propidium Iodide Assay.** Apoptosis was evaluated by the FCM assay using FITC-labeled Annexin V and propidium iodide (PI). The cells were seeded in 35 mm dishes (150,000 cells per dish) and allowed to attach overnight. After incubation with the LNPs as previously defined, the assay was carried out according to the manufacturer's protocol (Affimetrix, Vienna, Austria). Briefly, CTRL and treated MCF-7, MDA-MB-231, and MCF-7TAM cells were detached by trypsin treatment, washed by complete medium, and centrifuged at 1000 rpm for 5 min. After washing in PBS, the samples were re-suspended in 200  $\mu$ L of 1 $\times$  binding buffer. A total of 195  $\mu$ L was taken, and 5  $\mu$ L of Annexin V-FITC was added followed by 20 min incubation at room temperature. After washing and centrifuging, the cells were re-suspended in 195  $\mu$ L of 1 $\times$  binding buffer and 5  $\mu$ L of PI. Each sample was analyzed using an S3e Cell Sorter (BioRad, California, USA).

**Statistical Analysis.** Statistical analysis was performed using GraphPad Prism 6 Software (GraphPad Software Inc., San Diego, CA, USA). Data were expressed as mean  $\pm$  standard error (SE). Statistical significance was assessed using two-way ANOVA with a *p*-value (*p*) < 0.05 considered statistically significant.

## ■ ASSOCIATED CONTENT

### SI Supporting Information

The Supporting Information is available free of charge at <https://pubs.acs.org/doi/10.1021/acsomega.2c01829>.

(Figure S1) LNPs FITC and FA-LNPs FITC uptake in MCF10A cells; (Figure S2) Phasefocus Livecyte analysis of MCF10A cells growth (PDF)

Videos of cell growth (Video S1 (MCF-7); Video S2 (MDA-MB-231); and Video S3 (MCF-7TAM)) (ZIP)

## ■ AUTHOR INFORMATION

### Corresponding Author

Fulvia Farabegoli – FaBiT, Department of Pharmacy and Biotechnology, University of Bologna, 40126 Bologna, Italy;

[orcid.org/0000-0001-6254-9443](https://orcid.org/0000-0001-6254-9443);

Email: [fulvia.farabegoli@unibo.it](mailto:fulvia.farabegoli@unibo.it)

## Authors

Andreia Granja – LAQV, REQUIMTE, Departamento de Ciências Químicas, Faculdade de Farmácia, Universidade do Porto, 4050-313 Porto, Portugal

Joana Magalhães – LAQV, REQUIMTE, Departamento de Ciências Químicas, Faculdade de Farmácia, Universidade do Porto, 4050-313 Porto, Portugal; [orcid.org/0000-0001-9421-0444](https://orcid.org/0000-0001-9421-0444)

Stefania Purgato – FaBiT, Department of Pharmacy and Biotechnology, University of Bologna, 40126 Bologna, Italy

Manuela Voltattorni – FaBiT, Department of Pharmacy and Biotechnology, University of Bologna, 40126 Bologna, Italy

Marina Pinheiro – LAQV, REQUIMTE, Departamento de Ciências Químicas, Faculdade de Farmácia, Universidade do Porto, 4050-313 Porto, Portugal; Life and Health Sciences Research Institute (ICVS), School of Medicine, University of Minho, 4704-553 Braga, Portugal

Complete contact information is available at:

<https://pubs.acs.org/10.1021/acsomega.2c01829>

## Author Contributions

F.F. and M.P. designed the research. F.F., A.G., S.P., and M.V. performed the experiments, J.M. performed statistics, F.F. and M.P. wrote the manuscript, and F.F., A.G., M.P., and J.M. corrected and edited the manuscript. All authors have read and agreed the present version of the manuscript suitable for publication.

## Funding

This work was supported by the University of Bologna (RFO grant to Fulvia Farabegoli).

## Notes

The authors declare no competing financial interest.

## ■ ACKNOWLEDGMENTS

A.G. thanks FCT for the PhD grant SFRH/BD/130147/2017. M.P. thanks FCT for funding through program DL 57/2016 – Norma transitória.

## ■ REFERENCES

- (1) Cabrera, C.; Artacho, R.; Giménez, R. Beneficial effects of green tea—a review. *J. Am. Coll. Nutr.* **2006**, *25*, 79–99.
- (2) Chacko, S. M.; Thambi, P. T.; Kuttan, R.; Nishigaki, I. Beneficial effects of green tea: a literature review. *Chin. Med.* **2010**, *5*, 13–21.
- (3) Khan, N.; Mukhtar, H. Tea and health: studies in humans. *Curr. Pharm. Des.* **2013**, *19*, 6141–6147.
- (4) Khan, N.; Mukhtar, H. Tea Polyphenols in Promotion of Human Health. *Nutrients* **2019**, *11*, E39.
- (5) Yi, M.; Wu, X.; Zhuang, W.; Xia, L.; Chen, Y.; Zhao, R.; Wan, Q.; Du, L.; Zhou, Y. Tea Consumption and Health Outcomes: Umbrella Review of Meta-Analyses of Observational Studies in Humans. *Mol. Nutr. Food Res.* **2019**, *63*, e1900389.
- (6) Mereles, D.; Hunstein, W. Epigallocatechin-3-gallate (EGCG) for Clinical Trials: More Pitfalls than Promises? *Int. J. Mol. Sci.* **2011**, *12*, 5592–55603.
- (7) Yang, B.; Kensuke, A.; Kusu, F. Determination of Catechins in Human Urine Subsequent to Tea Ingestion by High-Performance Liquid Chromatography with Electrochemical Detection. *Anal. Biochem.* **2000**, *283*, 77–82.
- (8) Nakagawa, K.; Miyazawa, T. Chemiluminescence–High-Performance Liquid Chromatographic Determination of Tea Catechin,



- (–)-Epigallocatechin 3-Gallate, at Picomole Levels in Rat and Human Plasma. *Anal. Biochem.* **1997**, *248*, 41–49.
- (9) Chow, H. H.; Cai, Y.; Hakim, I. A.; Crowell, J. A.; Shahi, F.; Brooks, C. A.; Dorr, R. T.; Hara, Y.; Alberts, D. S. Pharmacokinetics and Safety of Green Tea Polyphenols after Multiple-Dose Administration of Epigallocatechin Gallate and Polyphenon E in Healthy Individuals. *Clin. Cancer Res.* **2003**, *9*, 3312–3319.
- (10) Del Rio, D.; Calani, L.; Cordero, C.; Salvatore, S.; Pellegrini, N.; Brighenti, F. Bioavailability and catabolism of green tea flavan-3-ols in humans. *Nutrition* **2010**, *26*, 1110–1116.
- (11) Naponelli, V.; Ramazzina, I.; Lenzi, C.; Bettuzzi, S.; Rizzi, F. Green Tea Catechins for Prostate Cancer Prevention: Present Achievements and Future Challenges. *Antioxidants* **2017**, *6*, E26.
- (12) Lazzeroni, M.; Guerrieri-Gonzaga, A.; Gandini, S.; Johansson, H.; Serrano, D.; Cazzaniga, M.; Aristarco, V.; Macis, D.; Mora, S.; Caldarella, P.; Pagani, G.; Pruneri, G.; Riva, A.; Petrangolini, G.; Morazzoni, P.; DeCensi, A.; Bonanni, B. A Presurgical Study of Lecithin Formulation of Green Tea Extract in Women with Early Breast Cancer. *Cancer Prev. Res.* **2017**, *10*, 363–370.
- (13) Stingl, J. C.; Ettrich, T.; Muche, R.; Wiedom, M.; Brockmüller, J.; Seeringer, A.; Seufferlein, T. Protocol for Minimizing the Risk of Metachronous Adenomas of the Colorectum with Green Tea Extract (MIRACLE): a randomised controlled trial of green tea extract versus placebo for nutripvention of metachronous colon adenomas in the elderly population. *BMC Cancer* **2011**, *11*, 360.
- (14) Bobo, D.; Robinson, K. J.; Islam, J.; Thurecht, K. J.; Corrie, S. R. Nanoparticle-Based Medicines: A Review of FDA-Approved Materials and Clinical Trials to Date. *Pharm. Res.* **2016**, *33*, 2373–2387.
- (15) Granja, A.; Vieira, A. C.; Chaves, L. L.; Nunes, C.; Neves, A. R.; Pinheiro, M.; Reis, S. Folate-targeted nanostructured lipid carriers for enhanced oral delivery of epigallocatechin-3-gallate. *Food Chem.* **2017**, *237*, 803–810.
- (16) Beloqui, A.; Solinís, M. Á.; Rodríguez-Gascón, A.; Almeida, A. J.; Prát, V. Nanostructured lipid carriers: Promising drug delivery systems for future clinics. *Nanomedicine* **2016**, *12*, 143–161.
- (17) Wang, S.; Low, P. S. Folate-mediated targeting of antineoplastic drugs, imaging agents, and nucleic acids to cancer cells. *J. Controlled Release* **1998**, *53*, 39–48.
- (18) Narmani, A.; Rezvani, M.; Farhood, B.; Darkhor, P.; Mohammadnejad, J.; Amini, B.; Refahi, S.; Abdi Goushbolagh, N. Folic acid functionalized nanoparticles as pharmaceutical carriers in drug delivery systems. *Drug Dev. Res.* **2019**, *80*, 404–424.
- (19) Granja, A.; Neves, A. R.; Sousa, C. T.; Pinheiro, M.; Reis, S. EGCG intestinal absorption and oral bioavailability enhancement using folic acid-functionalized nanostructured lipid carriers. *Heliyon* **2019**, *5*, No. e02020.
- (20) Corradini, A. G.; Cremonini, A.; Cattani, M. G.; Cucchi, M. C.; Saguatti, G.; Baldissera, A.; Mura, A.; Ciabatti, S.; Foschini, M. P. Which type of cancer is detected in breast screening programs? Review of the literature with focus on the most frequent histological features. *Pathologica.* **2021**, *113*, 85–94.
- (21) Neves, A. R.; Queiroz, J. F.; Costa Lima, S. A.; Figueiredo, F.; Fernandes, R.; Reis, S. Cellular uptake and transcytosis of lipid-based nanoparticles across the intestinal barrier: Relevance for oral drug delivery. *J. Colloid Interface Sci.* **2016**, *463*, 258–265.
- (22) Zhang, L.; Zhu, D.; Dong, X.; Sun, H.; Song, C.; Wang, C.; Kong, D. Folate-modified lipid-polymer hybrid nanoparticles for targeted paclitaxel delivery. *Int. J. Nanomed.* **2015**, *10*, 2101–2114.
- (23) Farabegoli, F.; Govoni, M.; Ciavarella, C.; Orlandi, M.; Papi, A. A RXR ligand 6-OH-11-O-hydroxyphenanthrene with antitumour properties enhances (–)-epigallocatechin-3-gallate activity in three human breast carcinoma cell lines. *Biomed Res. Int.* **2014**, *2014*, 853086.
- (24) Farabegoli, F.; Govoni, M.; Spisni, E.; Papi, A. EGFR inhibition by (–)-epigallocatechin-3-gallate and IIF treatments reduces breast cancer cell invasion. *Biosci. Rep.* **2017**, *37*, BSR20170168.
- (25) Gan, R. Y.; Li, H. B.; Sui, Z. Q.; Corke, H. Absorption, metabolism, anti-cancer effect and molecular targets of epigallocatechin gallate (EGCG): An updated review. *Crit. Rev. Food Sci. Nutr.* **2018**, *58*, 924–941.
- (26) Zalba, S.; Ten Hagen, T. L. Cell membrane modulation as adjuvant in cancer therapy. *Cancer Treat. Rev.* **2017**, *52*, 48–57.
- (27) Frandsen, S. K.; McNeil, A. K.; Novak, I.; McNeil, P. L.; Gehl, J. Difference in Membrane Repair Capacity Between Cancer Cell Lines and a Normal Cell Line. *J. Membr. Biol.* **2016**, *249*, 569–576.
- (28) Zhang, B. L.; Na, R.; Song, Y. F.; Mei, Q. B.; Zhao, M. G.; Zhou, S. Y.; Ye, W. L.; Du, J. B. Cellular uptake and antitumor activity of DOX-hyd-PEG-FA nanoparticles. *PLoS One* **2014**, *9*, No. e97358.
- (29) Donahue, N. D.; Acar, H.; Wilhelm, S. Concepts of nanoparticle cellular uptake, intracellular trafficking, and kinetics in nanomedicine. *Adv. Drug Delivery Rev.* **2019**, *143*, 68–96.
- (30) Necela, B. M.; Crozier, J. A.; Andorfer, C. A.; Lewis-Tuffin, L.; Kachergus, J. M.; Geiger, X. J.; Kalari, K. R.; Serie, D. J.; Sun, Z.; Moreno-Aspitia, A.; O’Shannessy, D. J.; Maltzman, J. D.; McCullough, A. E.; Pocka, B. A.; Cunliffe, H. E.; Ballman, K.; Thompson, E. A.; Perez, E. A. Folate receptor- $\alpha$  (FOLR1) expression and function in triple negative tumors. *PLoS One* **2015**, *10*, No. e0122209.
- (31) Scaranti, M.; Cojocaru, E.; Banerjee, S.; Banerji, U. Exploiting the folate receptor  $\alpha$  in oncology. *Nat. Rev. Clin. Oncol.* **2020**, *17*, 349–359.
- (32) Hansen, M. F.; Jensen, S. Ø.; Füchtbauer, E. M.; Martensen, P. M. High folic acid diet enhances tumour growth in PyMT-induced breast cancer. *Br. J. Cancer* **2017**, *116*, 752–761.
- (33) Tyagi, T.; Treas, J. N.; Mahalingaiah, P. K.; Singh, K. P. Potentiation of growth inhibition and epigenetic modulation by combination of green tea polyphenol and 5-aza-2'-deoxycytidine in human breast cancer cells. *Breast Cancer Res. Treat.* **2015**, *149*, 655–668.
- (34) Peter, B.; Bosze, S.; Horvath, R. Biophysical characteristics of proteins and living cells exposed to the green tea polyphenol epigallocatechin-3-gallate (EGCG): review of recent advances from molecular mechanisms to nanomedicine and clinical trials. *Eur. Biophys. J.* **2017**, *46*, 1–24.
- (35) Yang, C. S.; Wang, H.; Li, G. X.; Yang, Z.; Guan, F.; Jin, H. Cancer prevention by tea: Evidence from laboratory studies. *Pharmacol. Res.* **2011**, *64*, 113–122.
- (36) Yiannakopoulou, E. C. Effect of green tea catechins on breast carcinogenesis: a systematic review of in-vitro and in-vivo experimental studies. *Eur. J. Cancer Prev.* **2014**, *23*, 84–89.
- (37) Singh, B. N.; Shankar, S.; Srivastava, R. K. Green tea catechin, epigallocatechin-3-gallate (EGCG): mechanisms, perspectives and clinical applications. *Biochem. Pharmacol.* **2011**, *82*, 1807–1821.
- (38) Dai, W.; Ruan, C.; Sun, Y.; Gao, X.; Liang, J. Controlled release and antioxidant activity of chitosan and  $\beta$ -lactoglobulin complex nanoparticles loaded with epigallocatechin gallate. *Colloids Surf., B* **2020**, *188*, No. 110802.
- (39) Dube, A.; Nicolazzo, J. A.; Larson, I. Chitosan nanoparticles enhance the intestinal absorption of the green tea catechins (+)-catechin and (–)-epigallocatechin gallate. *Eur. J. Pharm. Sci.* **2010**, *41*, 219–225.
- (40) Radhakrishnan, R.; Kulhari, H.; Pooja, D.; Gudem, S.; Bhargava, S.; Shukla, R.; Sistla, R. Encapsulation of biophenolic phytochemical EGCG within lipid nanoparticles enhances its stability and cytotoxicity against cancer. *Chem. Phys. Lipids* **2016**, *198*, 51–60.
- (41) Pathak, Y.; Thassu, D. *Drug delivery nanoparticles formulation and characterization*. Vol. 191. 2016: CRC Press.
- (42) Granja, A.; Frias, I.; Neves, A. R.; Pinheiro, M.; Reis, S. Therapeutic Potential of Epigallocatechin Gallate Nanodelivery Systems. *Biomed. Res. Int.* **2017**, *2017*, 5813793.
- (43) Siddiqui, I. A.; Adhami, V. M.; Bharali, D. J.; Hafeez, B. B.; Asim, M.; Khwaja, S. I.; Ahmad, N.; Cui, H.; Mousa, S. A.; Mukhtar, H. Introducing Nanochemoprevention as a Novel Approach for Cancer Control: Proof of Principle with Green Tea Polyphenol Epigallocatechin-3-Gallate. *Cancer Res.* **2009**, *69*, 1712–1716.
- (44) Farabegoli, F.; Barbi, C.; Lambertini, E.; Piva, R. (–)-Epigallocatechin-3-gallate downregulates estrogen receptor alpha function in MCF-7 breast carcinoma cells. *Cancer Detect. Prev.* **2007**, *31*, 499–504.

(45) Kasproicz, R.; Suman, R.; O'Toole, P. Characterising live cell behaviour: Traditional label-free and quantitative phase imaging approaches. *Int. J. Biochem. Cell Biol.* **2017**, *84*, 89–95.